

BRIEF COMMUNICATION

Thermal Stability of $\text{Li}_4\text{Mn}_5\text{O}_{12}$ Electrodes for Lithium Batteries¹

M. M. Thackeray, M. F. Mansuetto, and C. S. Johnson

Electrochemical Technology Program, Chemical Technology Division, Argonne National Laboratory, 9700 South Cass Avenue, Argonne, Illinois 60439

Received June 3, 1996; accepted June 5, 1996

The thermal stability of the spinel, $\text{Li}_4\text{Mn}_5\text{O}_{12}$, which is of interest as an insertion electrode for 3 V lithium cells, has been studied by X-ray diffraction, differential thermal analysis, and thermogravimetric analysis at temperatures up to 1020°C. The data show that as the temperature is raised above 400°C, oxygen and lithia (Li_2O) are lost from the structure, which drives the composition of the spinel along the stoichiometric spinel tie-line from $\text{Li}_4\text{Mn}_5\text{O}_{12}$ toward Mn_3O_4 . By products of the reaction are the rock-salt phases Li_2MnO_3 at moderate temperature and LiMnO_2 at high temperature. The data are consistent with recent reports of the behavior of other lithium–manganese–oxide spinels; the data highlight, in particular, the sensitivity of lithium-rich spinels to temperatures above 400°C. © 1996 Academic Press, Inc.

© 1996 Academic Press, Inc.

INTRODUCTION

Lithium–manganese–oxide spinels are, currently, of scientific and commercial interest as insertion electrodes for rechargeable 3 V and 4 V lithium batteries (1–9). The stoichiometric spinels $\text{Li}_{1+x}\text{Mn}_{2-x}\text{O}_4$ ($0 \leq x \leq 0.33$), or in spinel notation $\text{Li}_{1+x}[\text{Mn}_{2-x}\text{Li}_x]_{\text{oct}}\text{O}_4$, are of particular significance. The spinels with low values of x ($0 \leq x \leq 0.1$) are of interest for 4 V lithium cells, whereas those with a high value of x are of interest for 3 V lithium cells (2, 7, 8). For instance, lithium is extracted from the tetrahedral sites in $\text{Li}_{1-y}[\text{Mn}_{2-x}\text{Li}_x]\text{O}_4$ at 4 V over the range $0 \leq y \leq 1 - 3x$, until the manganese oxidation state reaches 4. The cubic symmetry of the $\text{Li}_{1-y}[\text{Mn}_{2-x}\text{Li}_x]\text{O}_4$ structure is maintained throughout this reaction. Lithium insertion into $\text{Li}_{1+y}[\text{Mn}_{2-x}\text{Li}_x]\text{O}_4$ occurs at 3 V for the range $0 \leq y \leq 1$; in this reaction, the value of y is independent of x . When lithium is inserted into LiMn_2O_4 ($x = 0$), the elec-

trode is destabilized by the immediate onset of a Jahn–Teller distortion (i.e., when n_{Mn}^+ falls below 3.5); this reduces the crystal symmetry to tetragonal symmetry, resulting in a degradation of the structural integrity of the electrode and loss of cycling efficiency (1, 10). As the value of x increases in $\text{Li}_{1+x}\text{Mn}_{2-x}\text{O}_4$, so does the average oxidation state of the manganese ions. The electrochemical capacity that can be delivered by the spinel electrode at 4 V, therefore, decreases with x . At $x = 0.33$, the end member of the series is $\text{Li}_4\text{Mn}_5\text{O}_{12}$, in which all the manganese ions are tetravalent. Therefore, $\text{Li}_4\text{Mn}_5\text{O}_{12}$ offers no capacity at 4 V. However, in contrast to LiMn_2O_4 , $\text{Li}_4\text{Mn}_5\text{O}_{12}$ offers good electrochemical stability at 3 V because the onset of the Jahn–Teller effect occurs late in the discharge, when n_{Mn}^+ reaches 3.5, at $z = 2.5$ in $\text{Li}_{4+z}\text{Mn}_5\text{O}_{12}$ (2). As a result, $\text{Li}_4\text{Mn}_5\text{O}_{12}$ is an attractive electrode material for rechargeable 3 V lithium cells.

Recent reports have emphasized the difficulty of preparing $\text{Li}_{1+x}\text{Mn}_{2-x}\text{O}_4$ spinels with a predetermined stoichiometry (11–14) and that $\text{Li}_{1+x}\text{Mn}_{2-x}\text{O}_4$ spinels with high values of x are less stable to heat treatment than those with lower x values (15–17). We have undertaken a study of the thermal stability of $\text{Li}_4\text{Mn}_5\text{O}_{12}$ because of its importance as a 3 V electrode material. $\text{Li}_4\text{Mn}_5\text{O}_{12}$ products tend to be slightly nonstoichiometric and have an average manganese oxidation state slightly less than 4 (12–14). (For convenience, however, the spinel product that was fabricated for this investigation is referred to, simply, as $\text{Li}_4\text{Mn}_5\text{O}_{12}$.) We report analysis results from *in situ* high-temperature X-ray diffraction, thermogravimetric analysis (TGA), and differential thermal analysis (DTA) of $\text{Li}_4\text{Mn}_5\text{O}_{12}$. The data emphasize the sensitivity of lithium-rich spinels to moderate heat treatment.

EXPERIMENTAL

The spinel $\text{Li}_4\text{Mn}_5\text{O}_{12}$ was synthesized by the reaction of an intimately blended mixture of electrolytically prepared $\gamma\text{-MnO}_2$ (Chemetals) and $\text{LiOH} \cdot \text{H}_2\text{O}$ (Aldrich) in

¹ This article has been authored by a contractor of the U.S. Government under Contract W-31-109-ENG-38. The U.S. Government's right to retain a nonexclusive royalty-free license in and to the copyright covering this paper, for governmental purposes, is acknowledged.

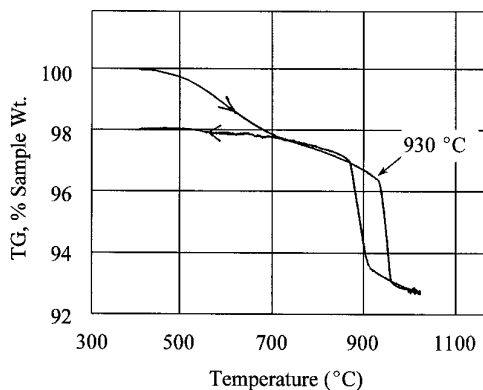


FIG. 1. The TGA plot of $\text{Li}_4\text{Mn}_5\text{O}_{12}$ (400 to 1020°C).

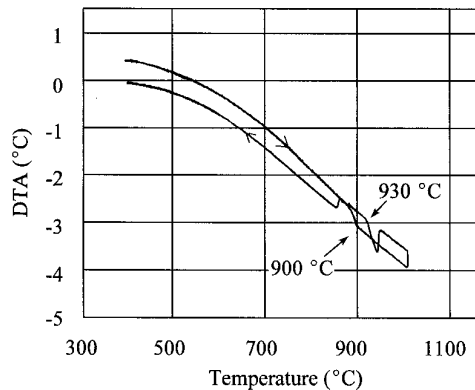


FIG. 2. The DTA plot of $\text{Li}_4\text{Mn}_5\text{O}_{12}$ (400 to 1020°C).

a 5:4 molar ratio. The mixture was heated in air at 600°C for 18 hours and cooled slowly in the furnace. The lattice parameter of the cubic unit cell of $\text{Li}_4\text{Mn}_5\text{O}_{12}$ was determined (1) by a least-squares refinement of the peak positions in the X-ray diffraction pattern ($a = 8.137(4)$ Å) and (2) by a profile refinement of the X-ray pattern (8.140(3) Å); the values fall within the range of those reported previously for $\text{Li}_4\text{Mn}_5\text{O}_{12}$ products (12–14).

Powder X-ray diffraction patterns were collected on a Siemens D5000 diffractometer. Data were collected *in situ* as the $\text{Li}_4\text{Mn}_5\text{O}_{12}$ sample was heated from room temperature to 1000°C using a Buhler HDK S1 high-temperature attachment. The sample was sprayed as a thin film onto a Pt/Rh heating strip and heated at 50°C intervals and allowed to equilibrate at each temperature before data collection. The scan speed of the diffractometer was $1.44^\circ 2\theta/\text{min}$; data were collected between 15 and $80^\circ 2\theta$.

The thermal stability of $\text{Li}_4\text{Mn}_5\text{O}_{12}$ was monitored from 400 to 1000°C by DTA and TGA techniques on a Netzsch STA 409 thermal analyzer. Approximately 100 mg of sample was used in these experiments. Alumina was employed both to contain the sample and to serve as a reference sample. The scan rate was 1°C/min on heating and cooling.

RESULTS AND DISCUSSION

TGA and DTA plots of $\text{Li}_4\text{Mn}_5\text{O}_{12}$ are shown in Figs. 1–3. The TGA plot for the temperature range 300 to 1020°C (Fig. 1) shows that $\text{Li}_4\text{Mn}_5\text{O}_{12}$ loses approximately 3.6% of its mass gradually between 420 (T_1) and 930°C, and a further 3.6% between 930 and 1020°C. The onset of a phase transition at 930°C (T_2) is associated with a rapid loss in mass from the sample. On cooling from 1020 to 400°C, the sample regains approximately 5.4% of the lost mass, which is attributed to the uptake of oxygen; the 1.8% net mass loss is attributed predominantly to evaporation of Li_2O from the sample. The DTA data in Fig. 2 confirm the transition at 930°C and show that the transition is

reversible, but with some hysteresis (onset temperature on cooling = 900°C). This behavior is similar to that observed in other $\text{Li}_{1+x}\text{Mn}_{2-x}\text{O}_4$ materials and is consistent with reports that T_1 is lowered significantly as the lithium concentration (x) in the spinel increases and that T_2 is relatively insensitive to x (6, 8). For example, T_1 and T_2 values for LiMn_2O_4 ($x = 0$), when heated in air, have been reported to be, respectively, 845 and 918°C (18), and 780 and 915°C (15).

The TGA plot of $\text{Li}_4\text{Mn}_5\text{O}_{12}$, when heated from 300°C to the original synthesis temperature ($\sim 620^\circ\text{C}$), is shown in Fig. 3. The plot confirms the onset of mass loss at 420°C and shows that even when heating to 620°C and slow cooling to 300°C, there is still an overall mass loss of 0.35% from the sample. It is unclear at this time whether this mass loss is due to evaporation of Li_2O from the sample or to an inability of the sample to fully regain lost oxygen on cooling under TGA conditions. Note the slight increase in mass that occurs on heating between 300 and 400°C (0.06%); it can be attributed to oxygen uptake and is further

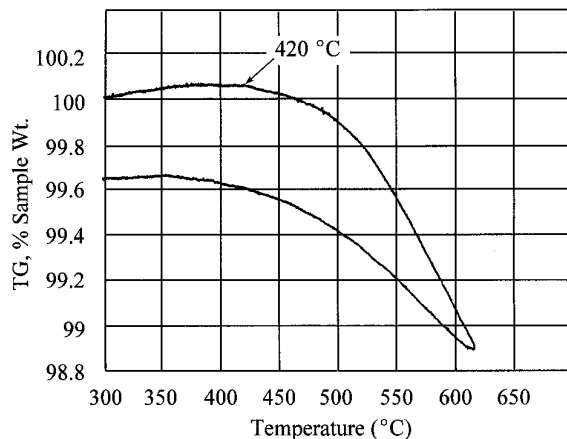


FIG. 3. The TGA plot of $\text{Li}_4\text{Mn}_5\text{O}_{12}$ (300 to 620°C).

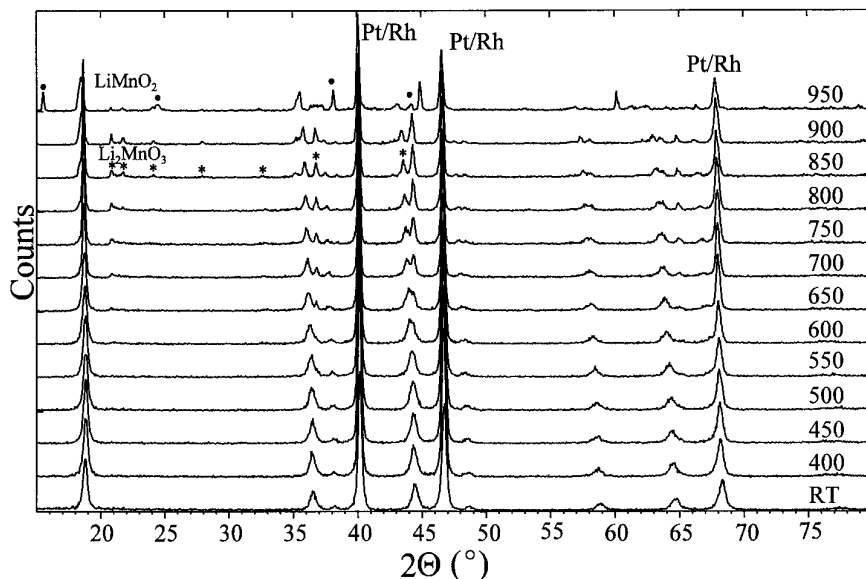


FIG. 4. X-ray diffraction profiles of a $\text{Li}_4\text{Mn}_5\text{O}_{12}$ sample recorded at temperatures between room temperature (RT) and 950°C. Characteristic peaks of Li_2MnO_3 (*) and LiMnO_2 (●) are indicated at 850 and 950°C, respectively.

evidence of the difficulty of preparing a spinel compound with the ideal $\text{Li}_4\text{Mn}_5\text{O}_{12}$ stoichiometry.

The powder X-ray diffraction patterns of $\text{Li}_4\text{Mn}_5\text{O}_{12}$, recorded at temperatures from room temperature (RT) to 950°C, are shown in Fig. 4. The onset of peaks due to a rock-salt Li_2MnO_3 phase at $\sim 21^\circ 2\theta$ can just be detected at 600°C; the concentration of Li_2MnO_3 in the sample increases as the temperature is raised to 900°C. A second rock-salt phase, LiMnO_2 , appears in the X-ray pattern at 950°C. These trends are consistent with those reported for heat-treated LiMn_2O_4 (4, 6, 15).

The combined TGA, DTA, and X-ray diffraction data therefore provide evidence that the following reaction processes occur when $\text{Li}_4\text{Mn}_5\text{O}_{12}$ is heated in air for the two temperature ranges 420–930°C and 930–1020°C. The reactions have been written for idealized situations, for simplicity.

420–930°C

The initial mass loss that occurs above 420°C (Fig. 1) is attributed to the loss of oxygen from the surface of the $\text{Li}_4\text{Mn}_5\text{O}_{12}$ particles. This reaction drives the composition of the spinel phase along the stoichiometric spinel tie-line $\text{Li}_{1+x}\text{Mn}_{2-x}\text{O}_4$ toward Mn_3O_4 (Fig. 5). This reaction reduces the manganese ions and lowers the Li:Mn ratio in the spinel phase. The surplus lithium diffuses rapidly to the particle surface where a stable lithium-rich rock-salt phase Li_2MnO_3 is formed. Note that the manganese ions are reoxidized at the surface and that no lithia is lost from the sample; it is contained on the particle surface as Li_2MnO_3

($\text{Li}_2\text{O} \cdot \text{MnO}_2$). A comparison of Figs. 1 and 4 indicates that the TGA data are more sensitive to the change in composition of the spinel electrode than the X-ray data, the latter showing the onset of the Li_2MnO_3 phase only at 600°C.

At higher temperatures in the 420–930°C range, lithia is irreversibly lost from the sample, as evident from the white lithia powder that could be detected in the sample chamber of the high-temperature attachment after the reaction. The exact temperature at which Li_2O starts to evaporate has not yet been unequivocally established. The TGA data in Fig. 1 show that the 3.2% mass which is lost on

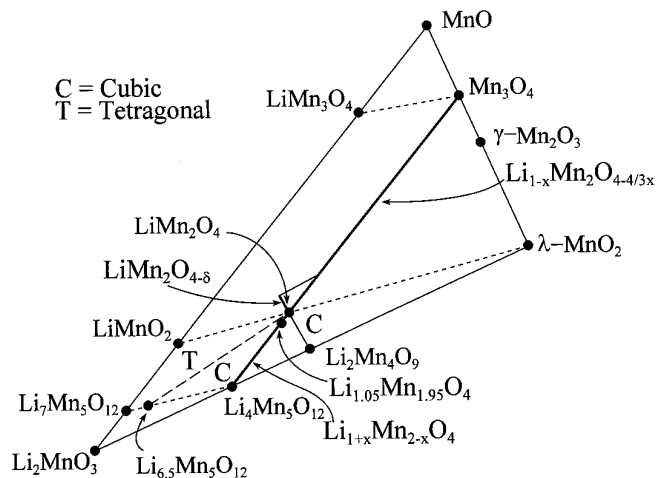
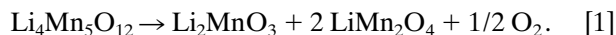


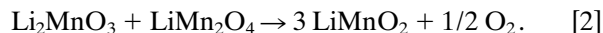
FIG. 5. A section of the Li–Mn–O phase diagram.

heating between 930 (T_2) and 1020°C is quickly recovered on cooling by the uptake of oxygen. This observation suggests that Li_2O is lost from the sample before T_2 is reached. If it is assumed that no Li_2O is lost from the sample until the spinel composition LiMn_2O_4 is reached, then the reaction to this point is simply

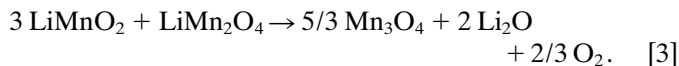


930–1020°C

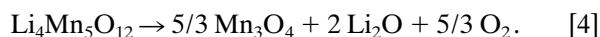
The XRD pattern recorded at 950°C (Fig. 4) indicates that the phase transition detected on the DTA plot at 930°C (T_2 in Fig. 2) is associated with the formation of the rock-salt structure LiMnO_2 . It is clear from the X-ray diffraction patterns at 900 and 950°C that the LiMnO_2 phase grows at the expense of the Li_2MnO_3 phase. The reaction between the rock-salt phase and the spinel phase generated by reaction (1) is



In reaction [2], the Li_2MnO_3 product generated by reaction [1] consumes only half of the available LiMn_2O_4 . Therefore, under this ideal situation, the products that would be left in the reaction vessel would be LiMnO_2 and LiMn_2O_4 in a 3:1 ratio. A previous study has shown that heating LiMn_2O_4 between 780 and 1200°C drives the composition of the spinel phase along the stoichiometric spinel tie line, designated $\text{Li}_{1-x}\text{MnO}_{4-4/3x}$ ($0 \leq x \leq 1$) in Fig. 5, from LiMn_2O_4 toward Mn_3O_4 , resulting in spinel phases with Mn^{2+} ions on the tetrahedral sites (15). By analogy, further heating of the products of reaction [2], if taken to completion, leads to



The overall reaction is



CONCLUSIONS

The results from this study stress the importance of temperature control when synthesizing $\text{Li}_4\text{Mn}_5\text{O}_{12}$ as an electrode material for 3 V lithium batteries; the data confirm that it is difficult to fabricate stoichiometric $\text{Li}_4\text{Mn}_5\text{O}_{12}$

and demonstrate that $\text{Li}_4\text{Mn}_5\text{O}_{12}$ products are unstable if heated above 400°C in air. An initial loss of oxygen from the spinel structure is accompanied by diffusion of lithium to the particle surface, which results in a surface film of electrochemically inactive Li_2MnO_3 . The formation of Li_2MnO_3 is undesirable because it not only reduces the capacity of the spinel electrode but also may limit access of lithium to the spinel particles. Further work is required to determine accurately the temperature limit to which $\text{Li}_4\text{Mn}_5\text{O}_{12}$ can be heated before Li_2O is irreversibly lost from the sample and to devise methods for fabricating completely oxidized (stoichiometric) $\text{Li}_4\text{Mn}_5\text{O}_{12}$ products in order to fully utilize the electrochemical capacity at 3 V.

ACKNOWLEDGMENT

Mark Hash is thanked for performing the TGA and DTA experiments.

REFERENCES

1. M. M. Thackeray, W. I. F. David, P. G. Bruce, and J. B. Goodenough, *Mater. Res. Bull.* **18**, 461 (1983).
2. M. M. Thackeray, A. De Kock, M. H. Rossouw, D. C. Liles, D. Hoge, and R. Bittihn, *J. Electrochem. Soc.* **139**, 363 (1992); also "Proceedings, Symposium on Primary and Secondary Lithium Batteries," Proc. Vol. 91-3, p. 326 1991.
3. T. Ohzuku, M. Kitagawa, and T. Hirai, *J. Electrochem. Soc.* **137**, 769 (1990).
4. J. M. Tarascon, E. Wang, F. K. Shokoohi, W. R. McKinnon, and S. Colson, *J. Electrochem. Soc.* **138**, 2859 (1991).
5. J. M. Tarascon, W. R. McKinnon, F. Coowar, T. N. Bowmer, G. Amatucci, and D. Guyomard, *J. Electrochem. Soc.* **141**, 1421 (1994).
6. A. Yamada, K. Miura, K. Hinokuma, and M. Tanaka, *J. Electrochem. Soc.* **142**, 2149 (1995).
7. R. J. Gummow, A. De Kock, and M. M. Thackeray, *Solid State Ionics* **69**, 59 (1994).
8. Y. Gao and J. R. Dahn, *J. Electrochem. Soc.* **143**, 100 (1996).
9. S. Megahed, and B. Scrosati, *J. Power Sources* **51**, 79 (1994).
10. M. M. Thackeray, *J. Electrochem. Soc.* **142**, 2558 (1995).
11. M. M. Thackeray and A. de Kock, *Mater. Res. Bull.* **28**, 1041 (1993).
12. T. Takada, H. Hayakawa, and E. Akiba, *J. Solid State Chem.* **115**, 420 (1995).
13. F. Le Cras, P. Strobel, M. Anne, D. Bloch, J.-B. Soupart, and J. C. Rousche, *Eur. J. Solid State Inorg. Chem.* **33**, 67 (1996).
14. C. Masqueller, M. Tabuchi, K. Ado, R. J. Kanno, Y. Kobayashi, Y. Maki, O. Nakamura, and J. B. Goodenough, "Proceedings, First Scientific Workshop on Electrochemical Materials, Osaka, Japan, 1996."
15. M. M. Thackeray, M. F. Mansuetto, D. W. Dees, and D. R. Vissers, *Mater. Res. Bull.* **31**, 133 (1996); also "Proceedings, International Battery Association Meeting, Chicago, Illinois October 7–8, 1995."
16. Y. Gao and J. R. Dahn, *J. Electrochem. Soc.* **143**, 1783 (1996).
17. Y. Gao and J. R. Dahn, *J. Appl. Phys.*, submitted.
18. Y. Gao and J. R. Dahn, *Appl. Phys. Lett.* **66**(19), 2487 (1995).